Dimuon Event Signatures in P-ONE Neutrino Telescope

by Louise Lallement Arnaud

MITACS summer internship
May 25, 2023 - August 18, 2023

Supervisor: Juan Pablo Yáñez

Host university:
University of Alberta
Department of Physics

Home university:
Université Grenoble Alpes
Master's degree of Subatomic Physics and Cosmology

Contents

1 Introduction

The Pacific Ocean Neutrino Experiment, or P-ONE, is a proposed neutrino telescope to be deployed off the coast of British Columbia, Canada. The project describes a multi cubic-kilometer Cherenkov detector designed to observe neutrino interactions at energies in the TeV-PeV range. The telescope's unique spatial and temporal resolutions will enable unprecedented identification of the products of these interactions. With P-ONE, physicists aim to investigate fundamental particle physics at the PeV scale and uncover previously unknown astronomical phenomena [1].

As of now, the primary institution at the forefront of high-energy neutrino astronomy research is the IceCube Neutrino Observatory, or simply IceCube, located at the geographic South Pole. With over 10 years of data, IceCube has led to major breakthroughs in both astro and particle physics. However, its size and resolution are limiting as larger neutrino statistics appear necessary to further explore developments in these two fields

Some of the neutrino interactions that will be closely studied in P-ONE are those which result in dimuon events. If it is typical for muon neutrinos to interact via deep inelastic scattering to produce a single muon, the Standard Model of particle physics also predicts that, in certain instances, a pair of closely spaced high-energy muons will be produced from the same neutrino interaction. This phenomenon is referred to as a 'dimuon'. The detection of these events in either IceCube or P-ONE can serve as a way to investigate rare Standard Model neutrino interactions and deviations in their rate could indicate the existence of physics beyond the Standard Model.

Sourav Sarkar, now a postdoctoral researcher at the University of Alberta, conducted an extensive analysis during his PhD thesis, examining over 10 years of IceCube data in pursuit of identifying dimuons. At the end of his research, Sourav identified a total of 4 candidates for dimuon events in IceCube 'against a background prediction of 2.13 events' [2]. However, the detector resolution and the scattering of light by the ice made it difficult to identify such events. That is why P-ONE, with its unique resolution and liquid water medium, holds great promise in the search of TeV- or PeV-scale dimuons.

During my 3-month internship with the P-ONE team at the University of Alberta, I was charged with running simulations to determine how many dimuon events the P-ONE telescope could be expected to observe. Sourav adapated his orginal programs to be able to use them in this new experiment and together we built a Monte Carlo-based event generator for a specific type of dimuon production, referred to as neutrino-induced charm dimuons.

2 A Word on P-ONE

Figure 1 presents the proposed instrumentation of P-ONE as of July 2021 [1]. It consists of 7 clusters of 10 mooring lines each, anchored to the ocean floor. Each line includes 20 optical modules, consisting of photomultiplier tubes (PMTs) able to detect the Cherenkov light emitted by relativistic particles as they propagate through water. The telescope is optimized for astrophysical neutrinos at energies in the TeV-PeV range.

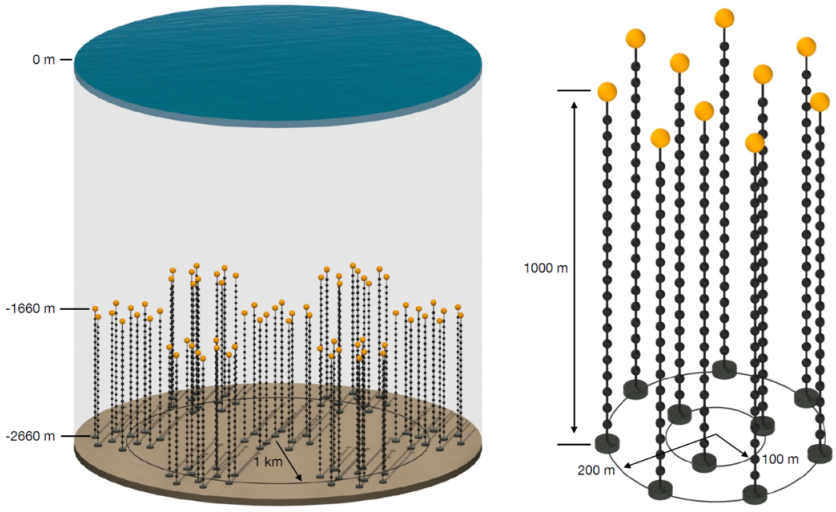

Figure 1: Design of the proposed instrumentation of P-ONE. The optimization process is currently in progress. *Left:* Complete telescope configuration, consisting of 7 clusters. *Right:* Single cluster, consisting of 10 mooring lines.

The telescope will be hosted by an existing oceanographic infrastructure, the NEPTUNE Observatory, operated by the Ocean Networks Canada and consisting of an 800-kilometer loop of fibre-optic in the Pacific Ocean. P-ONE will become part of a great network of neutrino telescopes with the IceCube Neutrino Observatory in Antarctica, KM3NeT in the Mediterranean Sea and Baikal-GVD in Russia. Together, these four detectors will cover both the northern and southern skies and push back the current limits of neutrino observation.

3 Charm Dimuon Production

3.1 Neutrino Deep Inelastic Scattering

In the Standard Model of particle physics, neutrinos are neutral leptons coming in three distinct flavors: electron, muon and tau. As they carry no electric nor color charge, neutrinos participate only in the weak interaction, via the exchange of a W or Z boson.

Charged current (CC) interaction occurs when an (anti)neutrino interacts via the exchange of a W boson to produce an outgoing charged lepton of the same flavor ($e^{\pm}$, $\mu^{\pm}$, $\tau^{\pm}$). The interaction of an (anti)neutrino of any type via the exchange of a Z boson is called neutral current (NC) and results in the production of an outgoing (anti)neutrino of the same flavor ($\nu_e(\bar{\nu_e})$, $\nu_\mu(\bar{\nu_\mu})$, $\nu_\tau(\bar{\nu_\tau})$). In P-ONE's energy range of interest ($E_\nu \geq 10$ GeV), both the W and the Z bosons couple to the individual quarks inside the target nucleons, resulting in an outgoing quark that can carry a large fraction of the incoming neutrino energy and leave the bound state of the target nucleon. The quark then undergoes the hadronization process to recombine with the rest of the nucleon, resulting in the production of several higher-energy outgoing hadrons. These interactions are known as neutrino deep inelastic scattering (DIS) and are shown below:

$$\begin{aligned} \text{CC DIS}: &\quad \nu_l(\bar{\nu}_l) + H \longrightarrow l^{\pm} + X, \\ \text{NC DIS}: &\quad \nu_l(\bar{\nu}_l) + H \longrightarrow \nu_l(\bar{\nu}_l) + X, \end{aligned}$$

where H is the target nucleon, X represents all the outgoing hadrons and $l = e$, μ, τ denotes the flavor of the process. 'The constituents of the hadrons are modelled using the quantum chromodynamics (QCD) framework and consist of real quarks (known as valence quarks) and virtual particle-antiparticle pairs (known as sea quarks and gluons). The interacting quark in the neutrino DIS interactions can come from either valence or sea quarks of the target nucleon' [2].

The study of neutrinos in P-ONE relies most heavily on the CC DIS interaction, where most of the incoming neutrino energy is deposited in the detector medium via the production of a charged lepton and multiple hadrons. The outgoing neutrino in the NC DIS interaction, on the other hand, escapes the detector without undergoing any additional interaction and only a fraction of the incoming neutrino energy is deposited in the medium via the jets of hadrons.

3.2 Charm Dimuon Event

The production of heavier quarks (charm, top) via neutrino CC DIS interaction requires incoming neutrinos of greater energies. Charm quark production is possible in the energy range under consideration in P-ONE ($m_{charm} = 1.3$ GeV/c^2) and occurs dominantly when an incoming muon neutrino interacts with a $d/s/b$ quark to produce an outgoing muon and a charm quark to undergo hadronization. The initial-state quark may be from either the valence (d) or sea (d, s, b) quarks of the target nucleon, with a negligible contribution of the b quark. A dimuon event results from the semileptonical decay of the resulting charm hadron into a second outgoing muon (∼10% of the time). The whole process is shown in Figure 2.

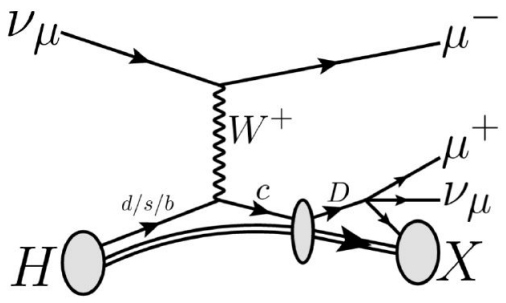

Figure 2: Feynman diagram showing neutrino-induced charm dimuon production. A muon neutrino interacts via CC DIS to produce a primary muon and a charm hadron, which decays into a secondary muon.

The primary muon from the CC DIS interaction and the secondary muon from the charm hadron decay can travel great distances in the detector, producing two long tracks and

creating a visible dimuon event signature. The two hadronic showers produced alongside each muon can also be observed in the form of 'cascade' tracks. These key features will allow the (somewhat tedious) identification of dimuon events in P-ONE.

It is important to note that subdominant processes exist within the Standard Model framework that can result in similar dimuon event signatures in the detector: Glashow resonance and neutrino trident production. The former occurs when an electron antineutrino interacts with an electron of the detector medium via s-channel CC. The latter requires that a neutrino interacts in the Coulomb field of a nucleus to produce two outgoing charged leptons, an outgoing neutrino and a recoiled nucleus. In his search for dimuon events in IceCube, Sourav only considered charm and trident dimuons. The objective of this work is to develop a generator for charm dimuons only.

4 Event Simulation

This work aims to determine the number of charm dimuon events that is expected to be detected in P-ONE. To accomplish this, we built a Monte Carlo-based event generator designed for simulating, weighing and subsequently quantifying such dimuon events in terms of event rates. The generator can be succinctly characterized as a sequence of five steps.

Figure 3 is a schematic representation of the sequence of processes involved in producing a charm dimuon event. The first three steps of the generator lie in simulating these processes to obtain such events: $\nu_\mu(\bar{\nu_\mu})$ CC DIS interaction and primary muon and charm quark production, hadronization, charm hadron decay and secondary muon production. The events are then weighted to reflect their probable occurrence given the true simulated quantities. Eventually, the particles are propagated through water and the detector volume in order to get double-track properties.

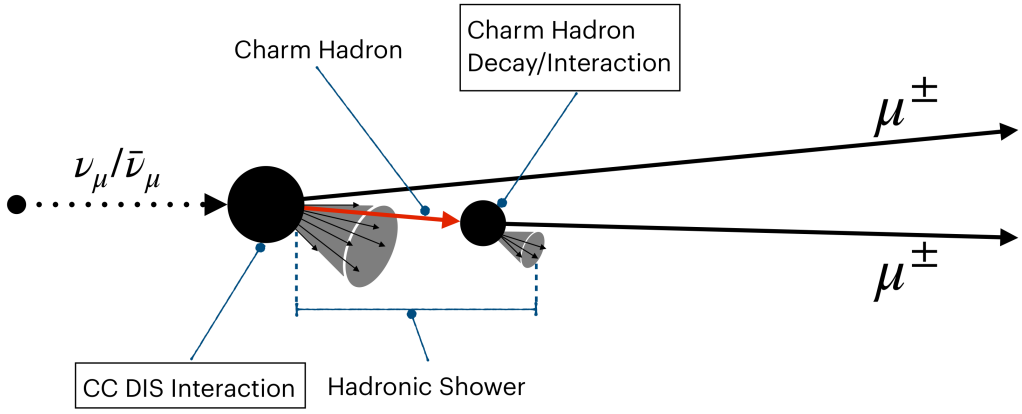

Figure 3: Intermediate processes involved in the production of a charm dimuon.

The five-step simulation is described hereinbelow in few details. For further explanations, please see Sourav's PhD thesis [2].

4.1 Energy and Geometry Sampling

The first step of the simulation is the random sampling of the incoming neutrino energy and direction. These properties are then used to build an injection volume centered on the detector to sample the interaction vertex. Using the `LeptonInjector` software package, a million events (500k neutrino events and 500k antineutrino events) are generated according to an arbitrary generation spectrum following a continuous power law:

$$\frac{\mathrm{d}N}{\mathrm{d}E} \propto E^{-\gamma},$$

with N the number of events, E the incoming neutrino energy and $\gamma = 1.5$ the spectral index. The events will eventually be weighted to achieve the desired Monte Carlo (MC) statistics. The incoming neutrino energies are sampled in the range 10^2 - 10^6 GeV. The simulation of the neutrino directions involves sampling angles from a zenith range (90° - 180°) and an azimuth range (0° - 360°). Figure 4 illustrates how to use these parameters to sample the interaction geometry.

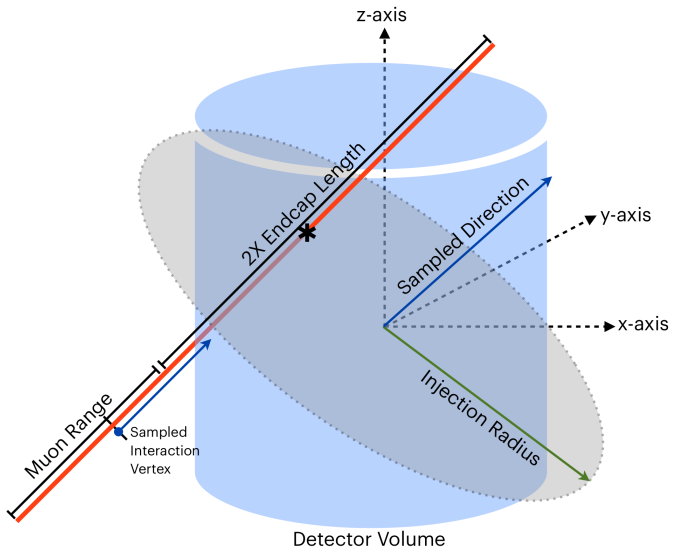

Figure 4: Diagram showing the sampling of the interaction geometry using `LeptonInjector`.

For each event, the sampled zenith and azimuth angles dictate the sampled direction and a circular disk is defined perpendicular to that direction at the center of the detector (with injection radius equal to 400 m). A point is sampled uniformly across the disk and, together with the direction, it defines the event's projected path. The maximum possible range for the outgoing muon is calculated (muon carrying the same energy as the incoming neutrino) and a safety length is added to the projected segment (twice the endcap length equal to 800 m). The interaction vertex of the simulated event is then evenly sampled as a position on the total segment (red line in Figure 4).

4.2 Primary Interaction and Hadronization

The second step consists of simulating neutrino CC DIS interactions with water and the hadronization of the produced charm quarks. The target nucleons are sampled according to their ratio in water: 10 protons and 8 neutrons per H_2O molecule. A target sampler program generates config files accordingly, containing the incoming neutrino energies from the first step and the sampled targets.

Using `PYTHIA` and `DIRE` framework and the said config files, a million $\nu_\mu(\bar{\nu_\mu})$ CC DIS interactions are simulated to produce outgoing muons and charm quarks followed by the hadronization process. The events are simulated in a vacuum, which is a good approximation since the detector medium does not impact the primary interaction and the hadronization as the processes occur on a short time scale.

4.3 Charm Hadron Decay and Interaction

In the third step, the charm hadrons are simulated to either decay semileptonically into a muon or interact in water before decay. The outgoing muon energy is sampled using a parametrization technique where the standalone decay of seven charm hadrons ($D^\pm$, D^0, $D_s^\pm$, $\Xi_c^\pm$, Ξ_c^0, $\Lambda_c^\pm$, Ω_c^0) is simulated by `PYTHIA` at multiple discrete energies. In order to assure the proper identification of the secondary muon from a muon in a hadronic shower, a 10 GeV cut is imposed on the muon energy.

4.4 Event Weight Calculation

The fourth step consists of assigning to each event an MC event weight (w_{MC}) in s^{-1}. It represents the probability of the event occurring given the true simulated quantities. The MC weight can be computed using a target neutrino flux model Φ_{target} (atmospheric or astrophysical fluxes) and a fluxless weight called $OneWeight$, constructed from different weight factors arising from each step of the simulation. The flux-dependent weight can be expressed as follows:

$$w_{MC} = OneWeight \times \Phi_{target},$$

and the $OneWeight$ is computed as:

$$OneWeight = \frac{w_{vol} \times w_{int} \times w_{prop}}{w_{gen} \times N_{events} \times N_{type}},$$

where:

- w_{vol} is the volume weight associated with the sampling of the interaction vertex. It depends on the total injection area in `LeptonInjector` and the solid angle over which the event position and direction are sampled.

- w_{int} is the interaction weight associated with the probability of the event. It depends on the total cross section of the dimuon event, the total interaction segment in `LeptonInjector` and the density of the material.
- w_{prop} is the propagation weight describing the probability of neutrinos traveling from the atmosphere and reaching the detector volume.
- w_{gen} is the generation weight associated to the generation spectrum. It depends on the neutrino energy of the simulated event and the energy range and spectral index γ used in the simulation.
- N_{events} is the total number of simulated events.
- $N_{type} = 0.5$ is the type factor introduced as half the events are neutrino events and half are antineutrino events.

Concretely, the output from `LeptonInjector` (which contains geometry information) is merged with the output from the previous step (which contains event kinematics) and the IceCube software, `IceTray`, is used to compute the $OneWeight$ from the resulting config file. The event rate of dimuon events can now be computed.

4.5 Daughter Particle Propagation

In the fifth and final step, the primary and secondary muons, as well as the two hadrons generated along the way, are propagated through water and the detector volume. The `PROPOSAL` software package is used for that purpose. The dimuon characteristic double-track properties can now be calculated.

5 Event Selection and Results

In total, 990,733 dimuon events were simulated, with incoming neutrino energy in the range 100 GeV - 1 PeV. A pre-existing cut stipulates that the energy of the secondary muon has to be ≥ 10 GeV. The simulation predicts a dimuon event rate of $1.734 \cdot 10^{-4}$ Hz in one P-ONE cluster. It corresponds to 54,697 expected events over a ten-year period.

Not all simulated events will be detectable in P-ONE due to the limitations in the detector's resolution. The PMTs on a string are about 50 m apart and the strings themselves are approximately 100 m apart at a minimum [1]. For a dimuon event to be identified, both muons need to travel far enough into the detector. It is also required that the muon tracks be distinguishable. In order to get a better appreciation of the rate at which dimuon events could be detected in P-ONE, MC cuts can be applied to the simulated data.

5.1 Cut Criteria

Let us denote the leading and trailing muons in a dimuon event as μ_1 and μ_2 respectively, following the condition that $E_{\mu_1} \geq E_{\mu_2}$, where E_{μ_i} is the energy of the muon. The track segments L_{μ_1} and L_{μ_2} correspond to the distance traveled by the muons inside the detector.

The highest track separation S_{max} corresponds to the lateral distance between the tracks when the trailing muon stops inside the detector or when both muons exit the detector. Figure 5 illustrates track segment and highest track separation.

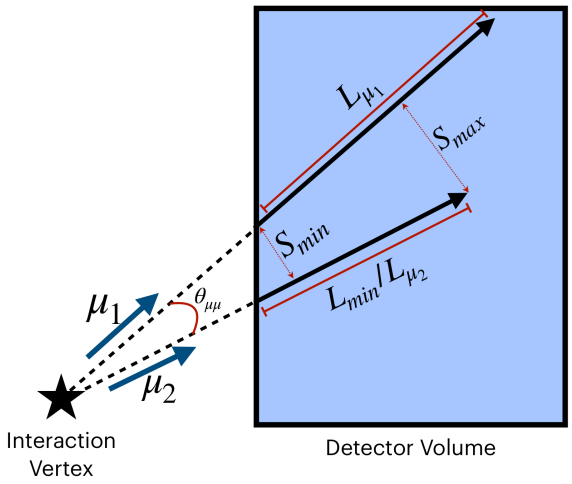

Figure 5: Illustration of the dimuon double-track with the leading muon track segment L_{μ_1}, the trailing muon track segment L_{μ_2} and the highest track separation S_{max}. The shortest track segment is also shown, denoted L_{min}.

Considering track segment and highest track separation, three cuts were applied to the generated dimuon events:

1. Minimum track segment $L_{min} > 200$ m

   Both muon tracks should be over 200 m. This assures that both muons are detected by several PMTs.

2. Maximum track segment $L_{max} > 200$ m

   Either muon track should be over 200 m. There is no guaranty that the trailing muon will travel very far into the detector.

3. Highest track separation $S_{max} > 25$ m & $L_{min} > 200$ m

   The highest track separation should be over 25 m. This assures that the tracks are distinguishable by the PMTs. Both muon tracks should also be over 200 m. This is the most restrictive selection criterion, but also that that assures the best identification of dimuons.

5.2 Particle and Double-Track Properties

Let us first look at some event properties. Figures 6 to 8 show event rate distributions as functions of some particle and double-track properties that can be helpful in checking that the dimuon events were properly simulated. Each graph includes the distribution for each of

the three cuts discussed hereinabove. I did not have time to add error bars, but the method to do so is discussed hereinbelow for future reference.

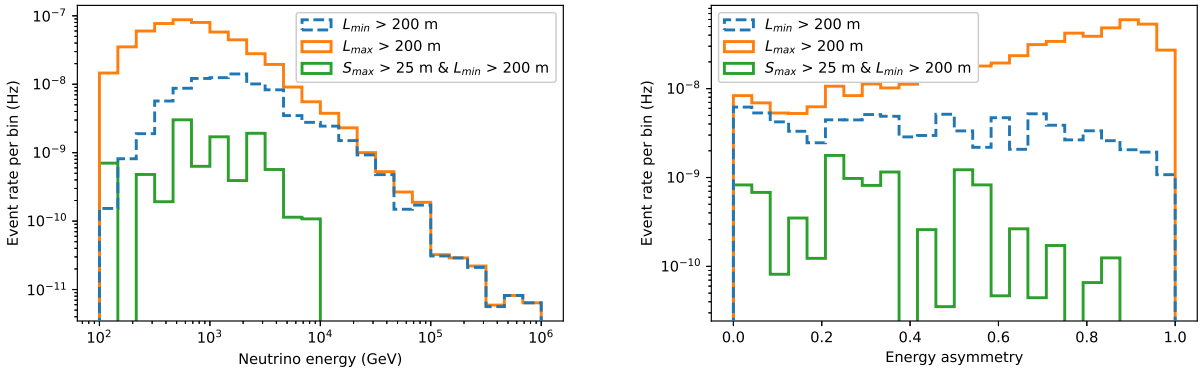

(a) (b)

Figure 6: Event rate distributions as a function of the incoming neutrino energy (a) and dimuon energy asymmetry (b).

Figure 6a presents the expected event rate distribution as a function of the incoming neutrino energy. At lower energies, the event rate is about one order of magnitude lower when we consider the minimum track cut (blue line) rather than the maximum track cut (orange line). However, the two cuts provide similar distributions at higher energies, since higher-energy neutrinos will produce longer dimuon double-tracks. As the subset of events that made the third cut consists of 53 events only, the statistical fluctuation does not allow to conclude much on the corresponding distribution (green line). That will be the case for all the graphs.

The energy asymmetry between the two muons μ_1 and μ_2 is defined as:

$$\text{Asymmetry} = \left| \frac{E_{\mu_1} - E_{\mu_2}}{E_{\mu_1} + E_{\mu_2}} \right|.$$

The corresponding event rate distribution is shown in Figure 6b. An asymmetry value close to 0 indicates that both muons have a similar energy ($E_{\mu_1} - E_{\mu_2} \approx 0$ if $E_{\mu_1} \approx E_{\mu_2}$). On the other hand, an asymmetry value close to 1 means that the energy of the leading muon is much larger than that of the trailing muon ($E_{\mu_1} - E_{\mu_2} \approx E_{\mu_1} + E_{\mu_2} \approx E_{\mu_1}$ if $E_{\mu_1} \gg E_{\mu_2}$). The distribution corresponding to the second cut (orange line) shows that the energy of the trailing muon can indeed be much lower than that of the leading muon. As the distance traveled in the detector depends directly on the particle energy, we can expect one of the muon track to stop well before the other in many dimuon events. This motivates the use of the first cut, which gives a relatively more homogeneous asymmetry distribution (blue line) by making sure that no track is too short.

This is also confirmed by Figure 7 which shows the event rate distributions as a function of the muon energies for the first and second cut. At higher energies, the event rate of the

leading muon (blue line) is up to one order of magnitude larger than that of the trailing muon (orange line). At lower energies (taking into account the 10 GeV cut on the secondary muon energy), the trend is reversed.

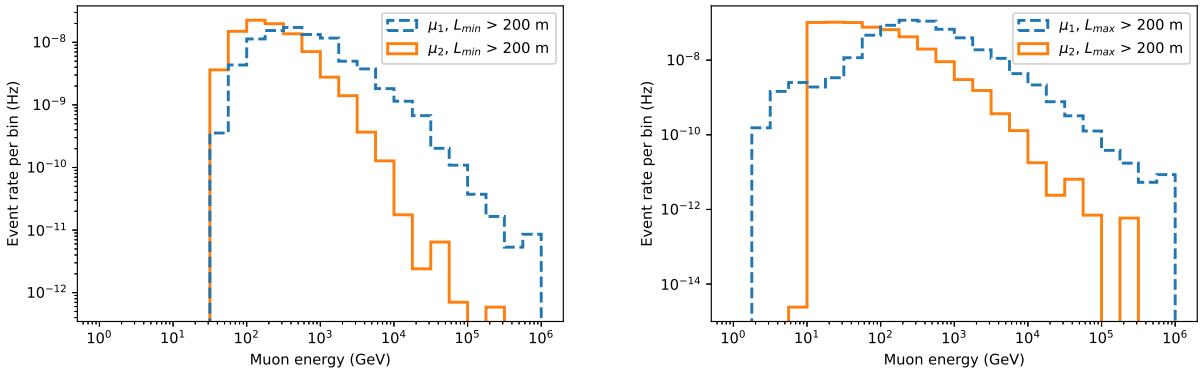

(a) (b)

Figure 7: Event rate distributions as a function of the muon energies for the first (a) and second cut (b).

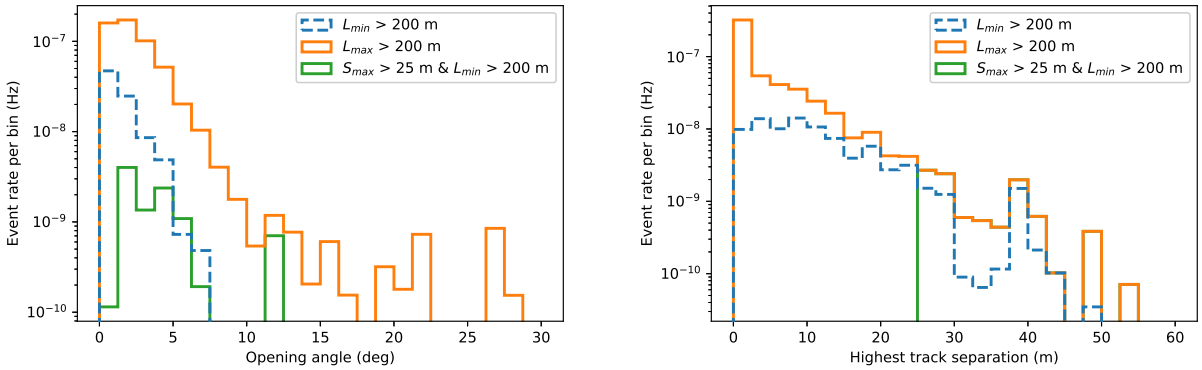

(a) (b)

Figure 8: Event rate distributions as a function of the opening angle between the two muons (a) and their highest track separation (b). On the second graph, the green line follows the orange line after 25 m.

Figure 8a presents the event rate distribution as a function of the opening angle between the two muons, which dictates the highest track separation. The corresponding event rate distribution is shown in Figure 8b. The statistical fluctuation is too important for the higher opening angles and larger track separations to really conclude anything. Figure 8b confirms that the dimuons with a highest track separation > 25 m also have both muons traveling far into the detector.

Before concluding this work, let us quickly explain how errors can be calculated here. If the event rate distribution is computed using the `NumPy` library and the weight denoted by the variable `w`: `n, _ = numpy.histogram(a, bins=10, weights=w)`, then the variance is given by: `var, _ = numpy.histogram(a, bins=10, weights=w**2)`. The standard deviation is then given by: `std = numpy.sqrt(var)`, and the 1-σ confidence interval on each value is: `[n - std, n + std]`.

5.3 Event Rates and Expected Events

Table 1 presents the event rates and expected events in 10 years depending on the selection criterion applied to the simulated data.

	No cut	Cut 1	Cut 2	Cut 3
No. of simulated events	990,733	1,105	4,109	53
Event rate (Hz)	$1.734 \cdot 10^{-4}$	$8.648 \cdot 10^{-8}$	$5.271 \cdot 10^{-7}$	$9.838 \cdot 10^{-9}$
Expected events (/10 y)	54,697	27.27	166.2	3.103

Table 1: Effect of the different cuts on the simulated event rates and corresponding expected events in 10 years. Let us recall that Cut 1 is $L_{min} > 200$ m, Cut 2 is $L_{max} > 200$ m and Cut 3 is $S_{max} > 25$ m & $L_{min} > 200$ m.

Figure 9 presents the distributions of event rates and expected events as functions of the minimum track segment and the highest track separation. The segment cut at 200 m and the separation cut at 25 m are included for better visualization of the above results. The plots indicate that approximately 0.005% of all simulated dimuons expected in one P-ONE cluster make the third and most restrictive cut ($S_{max} > 25$ m & $L_{min} > 200$ m).

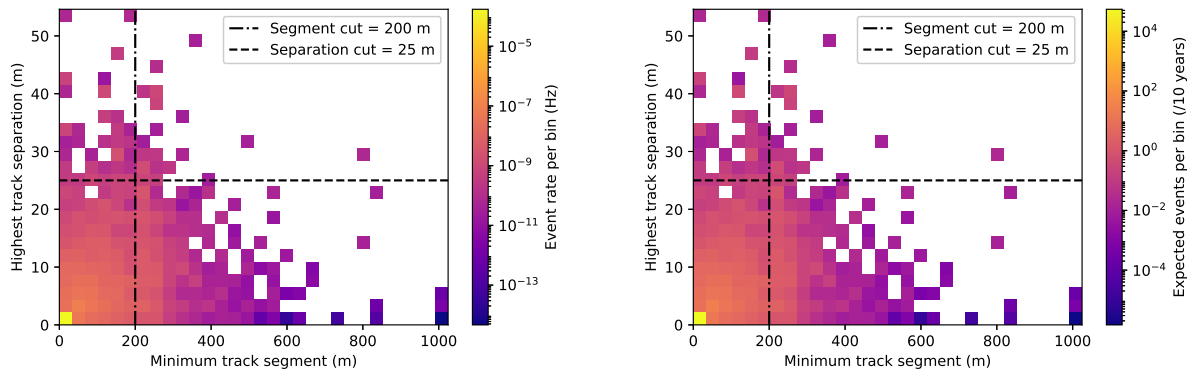

(a) (b)

Figure 9: Expected event rate (a) and expected events in 10 years (b) as functions of the minimum track segment and highest track separation. The two dash lines correspond to Cut 1 and Cut 3.

The whole charm dimuon generator and instructions to run it step by step can be found on my GitHub: `https://github.com/lallemel/CharmDimuon-Generator`, and in my Illume space: `\data\p-one\llallement\dimuon_generator`.

6 Conclusion

Through a Monte Carlo simulation and the application of specific event selection criteria, this work enabled the calculation of the expected event rates for neutrino-induced charm dimuon events in P-ONE. The results indicate that, while a substantial number of dimuon events are simulated, the implementation of stringent MC cuts reflecting the reality of neutrino detection significantly reduces the expected event rates. Nevertheless, even with the most restrictive criteria, it seems that P-ONE holds the potential to detect and study a non-negligible number of dimuon events over a ten-year period. It is important to keep in mind that the value of approximately 3 dimuons expected in 10 years with the condition $S_{max} > 25$ m & $L_{min} > 200$ m was calculated for one P-ONE cluster and that all event rates and expected events must be scaled up in order to best reflect the capacities of the telescope.

Overall, working on this project has been a very enriching and valuable experience. I took my first steps into the world of experimental research and learned a lot in physics simulation. Beyond meeting my initial learning objectives, this experience has broadened my horizons and opened exciting doors to future exploration in the field of neutrino astronomy. I extend my heartfelt gratitude to Juan Pablo Yáñez, Sourav Sarkar and the entire IceCube and P-ONE team at the University of Alberta for their unwavering support and guidance throughout this internship. I am looking forward to applying the knowledge and skills gained here to my forthcoming academic and professional pursuits in the world of particle physics.

References

[1] Elisa Resconi and P-ONE Collaboration. *The Pacific Ocean Neutrino Experiment*. 2021. arXiv: 2111.13133 [astro-ph.IM].

[2] Sourav Sarkar. "Search for TeV-Scale Neutrino Dimuon Events with 10.7 Years of IceCube Data". PhD thesis. University of Alberta, 2023. URL: https://github.com/ssarkarbht/PhDThesis.

Illustration Credits

Figure 1 Paper of Elisa Resconi and P-ONE Collaboration [1], Fig. 2.
Figure 2 PhD thesis of Sourav Sarkar [2], Fig. 2.5.
Figure 3 PhD thesis of Sourav Sarkar [2], Fig. 4.1.
Figure 4 PhD thesis of Sourav Sarkar [2], Fig. 4.2.
Figure 5 PhD thesis of Sourav Sarkar [2], Fig. 5.2a.